South American Journal of Herpetology, 16, 2020, 1–9

Histological Investigation of the Nile Crocodile (*Crocodylus niloticus*) Phallic Glans

Brandon C. Moore[1,*], Herman B. Groenewald[2], Jan G. Myburgh[3]

[1] *Biology Department, Sewanee: The University of the South. Sewanee, TN 37375, USA.*
[2] *Department of Anatomy and Physiology, Faculty of Veterinary Science, University of Pretoria. Onderstepoort 0110, South Africa.*
[3] *Department of Paraclinical Sciences, Faculty of Veterinary Science, University of Pretoria. Onderstepoort 0110, South Africa.*
[*] *Corresponding author. Email: bcmoore@sewanee.edu*

Abstract. The male crocodylian phallus, an intromittent organ, transfers sperm to the female cloaca during reproduction. During copulation, the distal phallic glans inflates via blood-filled spongiform tissues; it enlarges into an elaborate shape that directly interacts with the female urodeum—the cloacal chamber that contains the female reproductive tract openings. Alas, the specific mechanics of crocodylian insemination and gamete transfer remain unclear. To that end, we investigated the gross and cellular morphology of the Nile crocodile (*Crocodylus niloticus*) glans characterizing tissues types and structural morphologies to better predict how these male tissues may interact with those of the female. We tracked blood flow from the descending aorta to the phallic glans by way of sulcus spermaticus-adjacent blood vessels. Utilizing an artificial inflation technique, we documented how the glans tissue shape changes with increased hydrostatic pressure in spongiform tissues including increases in height and width and the enlargement of a cup-like distal lumen. Sectioning the glans, we traced the decrease in dense collective tissues and the proliferation of inflatable tissues moving from proximal to distal. Concomitant with the development of the inflatable glans, we identified elastin-rich tissues around the inflatable glans regions and the deep sulcus spermaticus semen conduit. Together, these observations demonstrated the dynamic nature of the tissues, where collagen fibers supply mechanical strength and elastin fibers provide resilience and recoil. We hypothesize how these glans characteristics may interact with female tissues during copulation to increase the chance of successful gamete transfer.

Keywords. Cloaca; Copulation; Crocodylian; Elastin; Inflation; Penis; Phallus; Reproduction.

INTRODUCTION

Male crocodylians use an intromittent organ during reproduction to transfer sperm to the female cloaca and ultimately the reproductive tract (Ziegler and Olbort, 2007; Grigg and Kirshner, 2015). At copulation, phalli of crocodylians, homologous to all vertebrate penises (Gredler, 2016), are mechanically everted from within the male cloaca (Kelly, 2013), and the exposed portion is comprised of a stiff proximal shaft and an inflatable distal glans (Moore et al., 2012). Upon intromission, the phallus moves through the female vent and enters the first chamber of the cloaca, the proctodeum. The static rigidity of phallic shaft assists achieving intromission, provides length to span the proctodeum, and internally acts as conduit for the semen through the sulcus spermaticus (Johnston et al., 2014; Moore and Kelly, 2015). Concomitantly, the dynamic glans of the penis inflates and elaborates to assume a complex copulatory shape (Johnston et al., 2014; Moore et al., 2016; Fitri et al., 2018) and interfaces with the middle chamber of the cloaca, the urodeum, which contains the oviductal openings and is the site of insemination (Kuchel and Franklin, 2000; Gist et al., 2008; Grigg and Kirshner, 2015). However, the biomechanics, anatomical specifics, and interspecies novelties associated with crocodylian male-to-female gamete transfer are unclear (Brennan et al., 2010; Kelly, 2016). Here, we work toward a better understanding of these tissue-to-tissue interactions that directly influence crocodylian reproductive success by characterizing the tissue types and architecture of juvenile male Nile crocodile (*Crocodylus niloticus* [Laurenti, 1768]) phallic glans and describing and measuring the changes in shape associated with copulation-specific inflation.

MATERIALS AND METHODS

Tissues were collected in May 2016 at Le Croc breeding farm and tannery near Brits, South Africa. Animal collection, handling, and tissue collection procedures conformed to South African and United States permitting and utilized Institutional Animal Care and Use Committee (IACUC) approved protocols.

Necropsy of n = 15 fresh male *Crocodylus niloticus* carcasses occurred soon after routine farm slaughtering. Animals were 2.0–3.0 years old with snout–vent lengths ranging from 87–101 cm. Phalli were photographed and

How to cite this article: Moore B.C., Groenewald H.B., Myburgh J.G. 2020. Histological investigation of the Nile crocodile (*Crocodylus niloticus*) phallic glans. *South American Journal of Herpetology* 16: 1–9. http://doi.org/10.2994/SAJH-D-18-00083.1

Submitted: 13 November 2018
Accepted: 25 February 2019
Available Online: 06 July 2020

Handling Editor: Carlos Piña
http://doi.org/10.2994/SAJH-D-18-00083.1

fixed in neutral buffered formalin with either flaccid or artificially inflated glans tissues before standard paraffin histological processing and microtome sectioning at 7 µm. Slides were stained using either Milligan's trichrome staining with aniline blue resulting in blue collagen, red nuclei, and red/purple muscles or Weigert's resorcin fuchsin resulting in purple elastin fibers with nuclear fast red counterstaining.

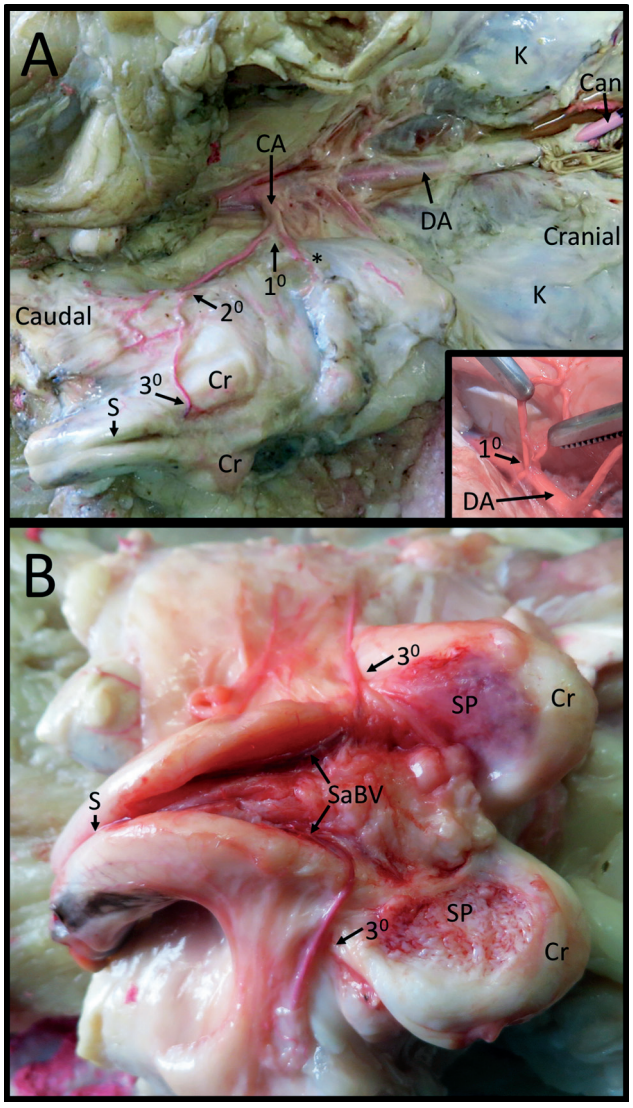

Figure 1. Necropsy of juvenile male *Crocodylus niloticus* with latex-injected cloacal and phallic vasculature. **(A)** Gross dissection of lower abdominal (right) and pelvic (left) region. Most of the cloaca and all of digestive tract has been removed and a flap of the phallus-containing region of the urodeum has been reflected toward the bottom of the image. Descending aorta (DA), cannula (Can), and kidneys (K). Arterial flow to the cloacal region: cloacal artery trunk (CA), first bifurcation (1^0) to opposing sides of the cloaca, second bifurcation (2^0) projects one artery to body of the urodeum while the other projects to the proximal origin of the phallic sulcus (S), third bifurcation (3^0) projects one vessel to the proximal crura (Cr) and the other to the distal phallic shaft and glans (removed in this picture). Inset: in one animal two distinct vessels (1^0) originated from the same region of the DA rather than as a single trunk. The asterisk marks the vessel cut during the dissection that profuse the contralateral side of the cloaca/phallus. **(B)** Gross dissection of the latex-injected crocodile phallus. Sulcus dissection widened the groove exposing the deeper tissues. Tissues overlying the crura were removed exposing the latex-filled supracrural plexuses (SP). A third vascular bifurcation (3^0) occurs on both sides of the phallic sulcus. The larger of the two diverging blood vessels projects distally, running adjacent to the medial sulcus (SaBV) to the distal glans while the smaller vessel project to the proximal spongiform tissues of the supracrural plexus overlying the cruca.

The inflation technique utilized is demonstrated in Video S1. The shaft of the necropsied penis was bisected and a needle was inserted into one of the two blood vessels flanking the sulcus spermaticus (gross anatomy presented in detail in Figure 1). The proximal phallic shaft was tied off with twine to impede fluid backflow through the contralateral blood vessel or other conduits. A syringe was used to inject neutral buffered formalin (NBF) into the tissue and the glans inflated with moderate constant fluid pressure. The syringe was held under pressure to maintain the inflation while the injected, pressurized fixative crosslinked the inflated tissues inside of the glans, thus maintaining an expanded shape. Following, the whole tissue was immersed in NBF to fix the external morphology. The sample shown in Video S1 was used for the gross and histological cross sections in Figures 3 and 4, respectively.

Height and width caliper measures of three phalli were made at the narrowest aspect of the shaft and the widest aspect of the glans before and again after inflation (Fig. 2A–B). The average percentage changes of each measure were calculated, and the values before and after inflation were compared using paired samples *t*-tests.

Three carcasses were transported to Faculty of Veterinary Science, University of Pretoria for investigation of cloacal/phallic arterial blood flow. The abdomen was dissected and red liquid latex was injected via a cannula into the descending aorta inserted between the kidneys (Fig. 1). During latex injection, phallic profusion was confirmed by observing red latex leaking from the distal phallic shaft where the glans had been previously removed. The latex was allowed to solidify over three days as animals were stored under refrigeration before dissection of the cloaca and male genitalia vasculature.

RESULTS

Cloacal and phallic blood flow

Dissection of latex-injected crocodile vasculature revealed the source of blood flow to the phallus. Arterial flow from the aorta begins as either as a single short (a few centimeters) cloacal artery trunk before a first bifurcation or, as in one of three animals, two distinct vessels originating from the same region of the aorta (Fig. 1A and inset). Each of the two vessels of the first bifurcation profuse a single respective side of the cloaca and phallus. For each of these vessels, a second bifurcation on each side of the cloaca projected one artery to profuse the body of the urodeum while the other projected to the proximal origin

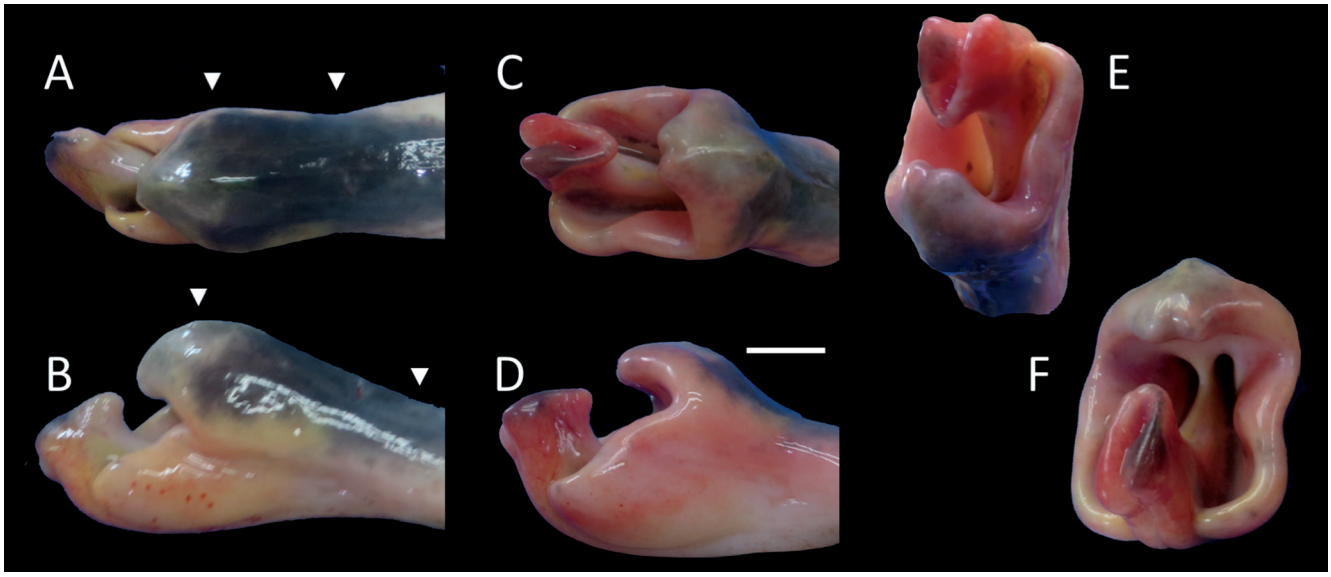

Figure 2. *Crocodylus niloticus* glans and distal phallic shaft **(A–B)** before and **(C–F)** after artificial inflation. **(A, C)** Tissue face opposite the sulcus spermaticus. **(B, D)** Lateral view. **(E, F)** Views of the glans lumen with internal medial septum after inflation. White triangles in A, B show the representative sites of caliper measures before and after inflation with data presented in Table 1. Scale bar = 1 cm.

of the phallic sulcus. A third bifurcation of the phallic-directed artery projected one vessel to the proximal crura and the other distal to the phallic shaft and glans. Further dissection of the sulcus and crura exposed the destination of these vessels. The smaller of the two vessels led to the crura and perfused a supracrural plexus, spongiform vascular tissues overlying the dense, collagen-rich crura. The larger of the two diverging blood vessels projected toward the distal phallus, running through the shaft adjacent to the medial sulcus spermaticus toward the distal glans.

Glans morphology

The Nile crocodile glans has a complex shape and a dynamic, but currently ill-defined reproductive function. In flaccid state, the glans has a greater height and width than the phallic shaft (Table 1), and these measures are greater at a protruding lip of glans tissue termed the phallic ridge or cuff (Fig. 2B). Considering the phallic ridge as dorsally placed, the sulcus spermaticus runs along the ventral aspect of the tissue and terminates in an upturned blunt glans tip (Fig. 2A–B) that extends more distally than the end of the phallic ridge. Together, the glans ridge, lateral glans faces, and ventral sulcus region define a lumen with a distally facing opening that is partially collapsed when the glans is flaccid.

With inflation, glans morphology substantially changes (Video S1). Inflation predominantly enlarged the lateral faces of the glans; they expanded outwards and become more ridged with the growing internal pressure. This, in turn, enlarged the glans lumen and produced a prominent notch at the interface of the lateral glans and the glans ridge (Fig. 2C–F). The glans tip also expanded (but did not elongate) with the most distal aspect assuming a V-shaped fossa at the termination of the sulcus groove (Fig. 2C, E–F). The ventral tissues of the glans containing the sulcus, in part, formed a medially placed vertical septum in the deeper aspects of the lumen that became visible with inflation (Fig. 2E–F). Inflation also made a raised crest running along the glans cuff midline ending at a small cleft in the distal lip of the glans ridge more prominent (Fig. 2E–F). On average, inflation resulted in minor increases in shaft height (+ 7%) and width

Table 1. Caliper measures (cm) of necropsied crocodile phalli before and after experimental inflation. Measures were performed first at the thinnest parts of the shaft and the widest parts of the glans before inflation and at the same spots after inflation (sites denoted by white arrowheads in Figure 2).

Sample	Snout–vent length	Flaccid shaft height	Inflated shaft height	% increase	Flaccid shaft width	Inflated shaft width	% increase	Flaccid glans height	Inflated glans height	% increase	Flaccid glans width	Inflated glans width	% increase
1	93	1.30	1.40	7.7	1.30	1.50	15.4	2.00	2.70	35.0	1.50	2.40	60.0
2	96	1.30	1.35	3.8	1.30	1.40	7.7	1.50	2.30	53.3	1.45	2.20	51.7
3	96	1.00	1.10	10	1.15	1.30	13.0	1.40	1.90	35.7	1.25	2.0	60.0
Average		**1.20**	**1.28**	**7.2**	**1.25**	**1.40**	**12.0**	**1.58**	**2.33**	**41.3**	**1.45**	**2.17**	**57.2**
Paired *t*-test		***P* = 0.038**			***P* = 0.035**			***P* = 0.017**			***P* = 0.004**		

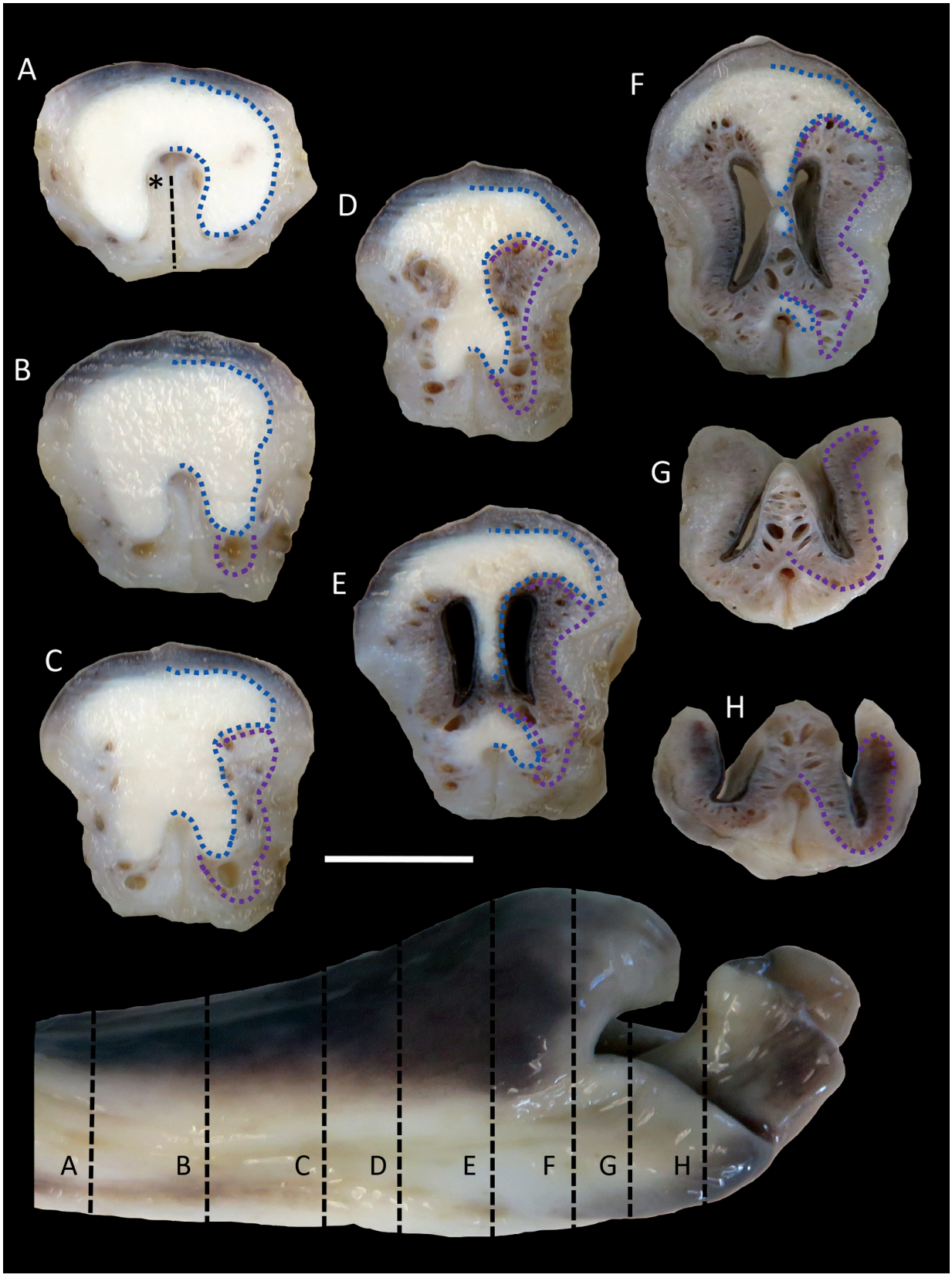

Figure 3. Gross cross-sections of an inflated *Crocodylus niloticus* glans after inflation. Vertical dotted lines on the intact tissue at the bottom denote the location of sections A–H. **(A)** The phallic shaft in cross-section. The asterisk shows the location of one of the two sulcus-adjacent blood vessels used for glans inflation (see technique in Supplemental Video 1). The black dotted line denotes the location of the sulcus spermaticus. **(A–F)** Blue dotted lines delimit hemi-sections of dense, collagen-rich connective tissues. **(B–H)** Purple dotted lines delimit hemi-sections of spongiform tissues. Scale bar = 1 cm.

(+ 12%) and more sizable changes in glans height (+ 43%) and width (+ 57%). The glans height increase was derived from an elevation of the ridge as the lateral faces expanded (compare Fig. 2B and D).

Transverse gross sectioning of inflated phalli revealed internal structures that regulate glans function and expansion. A central region of dense connective tissues in the phallic shaft presents as a white horseshoe shape around the ventro-medial sulcus spermaticus (Fig. 3A). The semen conduit of the sulcus is placed roughly in the middle of the shaft. As the phallus morphology transitions from shaft to glans, the dense connective tissue widens dorsally and narrows laterally (Fig. 3B–C). Concomitantly, the sulcus groove becomes shallower, the semen conduit is more ventrally placed, and the middle of the phallus contains dense connective tissue. Continuing distally in the glans, increasing amounts of spongiform tissues are observed on the lateral sides of the dense connective tissue core (Fig. 3C–D). The lumen develops on the lateral sides of the narrowing medial dense connective tissue, that is now in part comprising the medial septum dividing the deep lumen (Fig. 2E). The dorsal aspect of the distal glans ridge is comprised by a wide crescent of dense connective tissues. Spongiform tissues are found ventro-lateral to the luminal spaces. Further distally, the ventral part of the luminal septum is replaced by inflatable tissues, but a small arc of dense connective tissues continues to surround the dorsal aspect of the semen conduit (Fig. 3F). After the glans ridge terminates, the glans tip continues distally and curves medially. It contains the ventrally placed sulcus beneath a W-shaped spongiform tissue region (Fig. 3G–H) the center of which continued to the V-shaped terminus of the glans tip.

Glans histology

Histological sectioning and staining of glans tissues further characterizes dynamic structures associated with inflation. The groove of the sulcus spermaticus is flanked along its length on both sides by smooth muscle fiber bundles in radial parallel orientations (Fig. 4A–D, Fig. 5D). As the phallic shaft transitions to the glans, folds of the stratified squamous epithelia (Fig. 5B) begin to be observed on the lateral faces (brackets in Fig. 4A–C, in detail Fig. 5A). These folds overlie ventro-lateral regions of spongiform, inflatable tissues. Some folds show putative infection sites where the involuted mucosal epithelium is eroded (Fig. 5A) and lymphocyte aggregates fill the subjacent connective tissues (Fig. 5C).

The dense connective tissues seen in the gross glans cross sections present histologically as comparatively robust collagen fiber bundles with multidirectional orientations (Fig. 4A–C). These dense tissues predominate the glans ridge spanning the dorsal aspect of the glans and

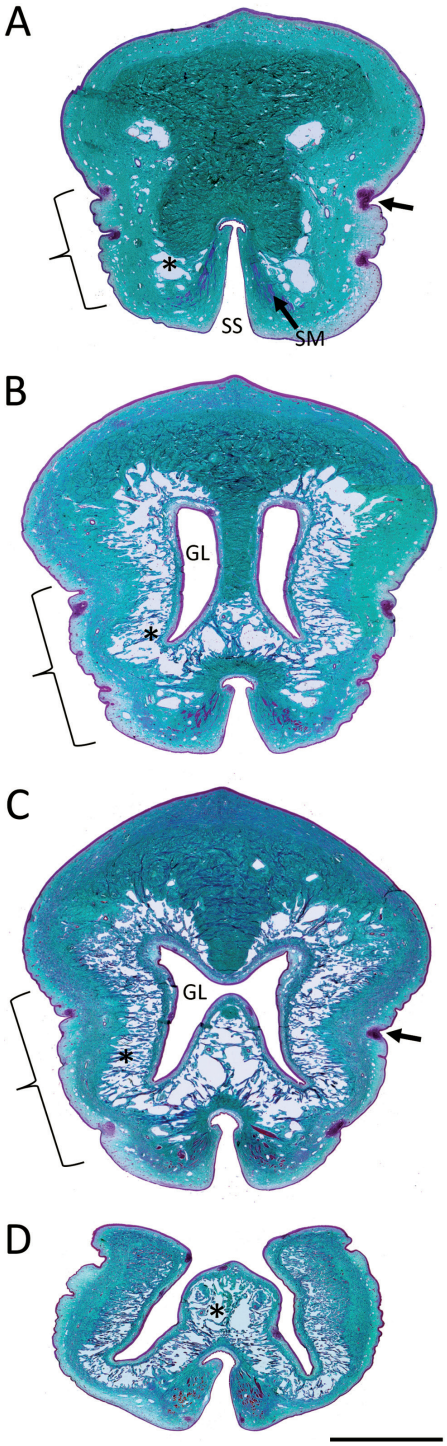

Figure 4. Histological cross-sections of selected inflated glans tissues in Figure 3. Images A–D approximately correspond to gross dissection images in Figure 3C, E, F, H, respectively. Brackets define ventro-lateral regions of folded epithelium overlying spongiform inflatable tissues (asterisks) that are first observed in the proximal glans in A and more distally circumscribe the glans lumen (GL) in B and C. Some epithelial folds present lymphocyte aggregates (arrows), cells staining red against blue/green stained connective tissues. The ventral sulcus spermaticus (SS) is flanked by red/purple staining, parallel-oriented smooth muscle fiber bundles (SM) in all sections. Note: the open sulcus groove observed in the histological sections is a processing artifact. Compare sulcus morphologies to Figure 3. Milligan's Trichrome. Scale bar = 0.5 cm.

the septum dividing the lumen. In histological section, the raised crest running the length of the medial glans ridge is apparent. Spongiform, inflatable tissues are prevalent in the lateral faces and ventral to the glans lumen. Dorsally, inflatable tissues are bisected by the dense connective tissue lumen septum (Fig. 4B–C). Trabecula of fine connective tissues span the inflatable spaces throughout the whole glans ridge and tip. Small aggregates of red blood cells are observed throughout the spongiform tissue sections (Fig. 6A, C).

Histochemical elastin staining highlighted glans tissues that undergo stretching with inflation and therefore require pliable and resilient biomechanical properties. The inflatable region of the glans is bounded on both the outer and luminal sides by elastin-rich irregular connective tissues (Fig. 6A–B). The outer elastin-rich region is comparatively thicker than the inner elastin-rich region adjacent to the glans lumen. Additionally, the trabeculae of the spongiform tissues are also intercalated with elastin fibers, but they present as more gracile and sparser in comparison (Fig. 6C). Elastin fibers were also observed on the inner face of the dense connective tissues surrounding the branched and folded epithelium of the semen conduit of the sulcus spermaticus (Fig. 6D).

DISCUSSION

The crocodile phalli of this study showed size and pigmentation variation among animals, but minimal variation in overall form between samples before and after inflation. Application of the inflation technique resulted in a predictable glans morphology with conserved features on the glans ridge, lumen, and glans tip. This homogeneity is consistent with a hypothesis that the glans shape and its physical properties play a distinct role while interacting with female tissues during copulation and facilitating effective gamete transfer. While the overall structure of

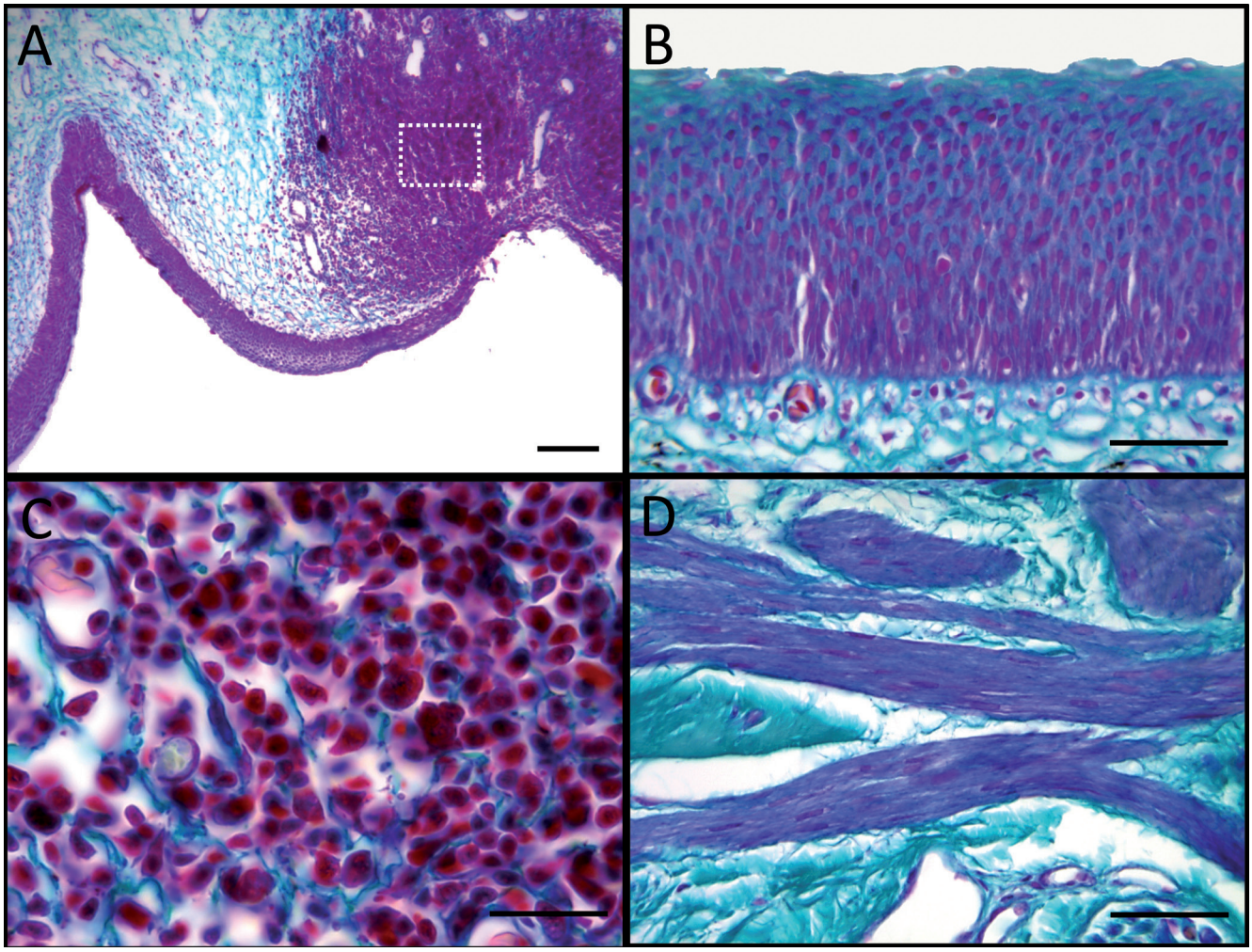

Figure 5. Detail images of glans features from Figure 4. **(A)** Glans epithelium showing a lateral fold in the normal morphology (left) and adjacent lesioned tissues with eroded epithelium (right). **(B)** Stratified squamous epithelium of the glans and subjacent collagen fiber-rich tissues (blue). **(C)** Detail of inset box in A. Lymphocyte aggregate are intercalated into connective tissues. **(D)** Smooth muscle fiber bundles in dense irregular connective tissues that run parallel on both sides of the sulcus spermaticus epithelia (not shown). Milligan's Trichrome. Scale bars: A = 100 µm, B–C = 50 µm.

female crocodylian cloacal chambers and associated oviducal openings have been described, the dynamic interaction with male phalli during reproduction is currently unstudied and not in the scope of this study. However, from this characterization of male phallic anatomy we can make inferences and predictions laying a foundation for further male-female tissue interaction study.

The inflation technique employed in this study provides strong evidence of a vascular glans inflation. We tracked blood flow from the aorta to the glans and observed blood cell aggregates in spongiform tissues. The technique also showed a single contiguous inflatable space in the glans body and around the ventral sulcus that is independently served by two arteries, wherein fluid

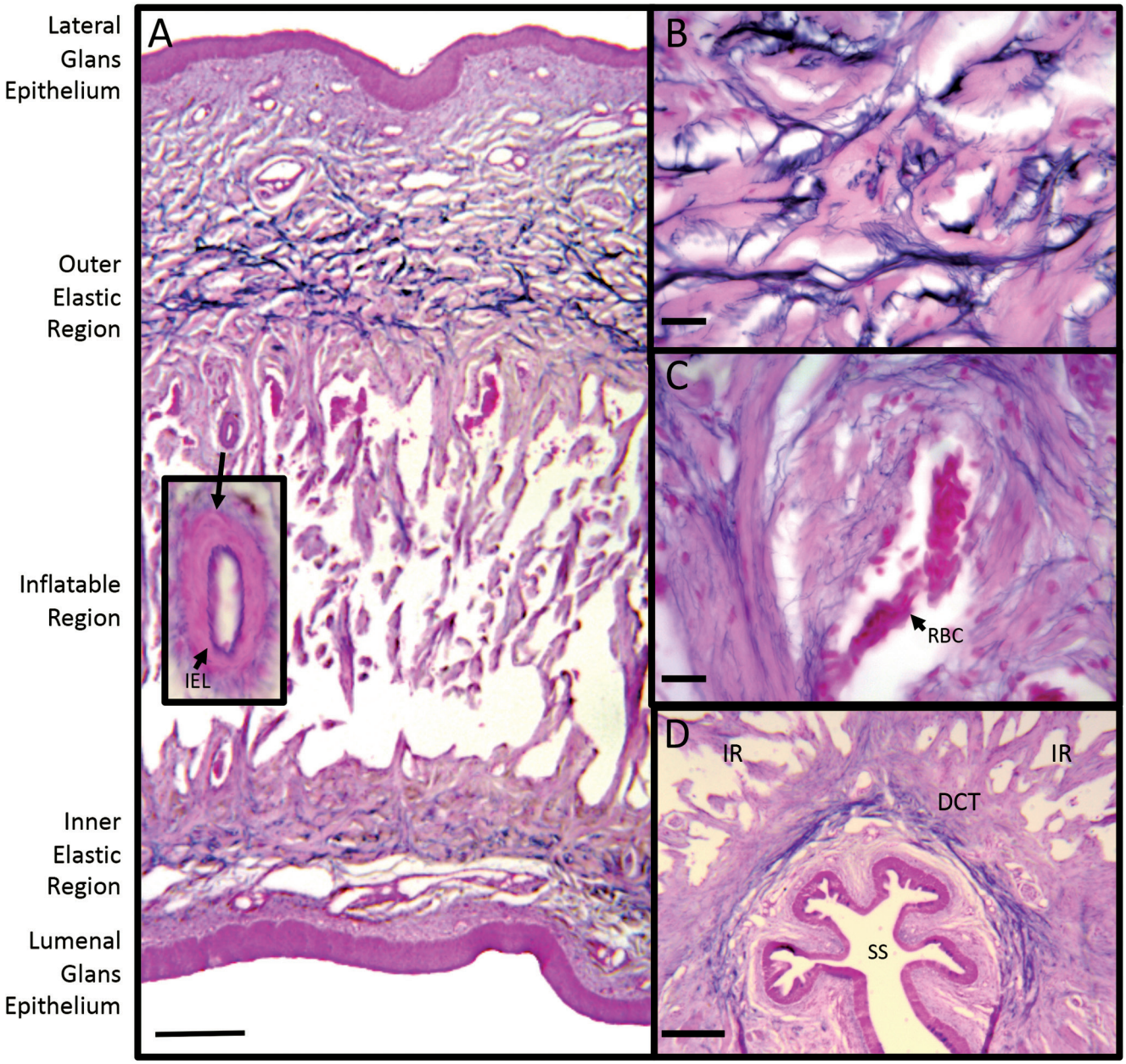

Figure 6. Elastin histochemistry of the *Crocodylus niloticus* glans. Elastin fibers stain blue/purple against a nuclear fast red counterstain. **(A)** A representative cross-section of the distal glans spanning from the inward/medial glans lumen tissue face to the outward/lateral glans face. While this cross-section is relatively thin, the morphology of the layers is representative of those found throughout the entire inflatable glans. A medially placed inflatable region of spongiform tissues is bounded by inner/thinner and outer/thicker regions of dense, more elastin-rich irregular connective tissues. Elastin fiber bundles of the inflatable region are finer and less numerous than the elastic regions. The inset figure shows the positive elastin staining of an arteriole inner elastic lamina (IEL). **(B)** Detail of elastin fibers in the outer elastic region. **(C)** Detail of the inflatable region showing red blood cell aggregates (RBC) observed throughout the tissue (see A). **(D)** Elastin fiber bundles circumscribe the sperm conduit of the deep sulcus spermaticus (SS). In the more distal glans, the deep sulcus is immediately bounded by a crescent of dense connective tissue (DCT, also note Figure 2E, F) with an elastin-rich internal layer and externally bounded by the inflatable tissue region (IR). Scale bars: A, D = 200 μm, B, C = 50 μm.

pressure from either conduit equally inflates the glans. The venous return system or how vascular constriction during intromission may maintain/maximize glans inflation is not yet understood.

With the morphological insight from these results, we can better speculate on the role of glans shape and physical properties in copulation. The female proctodeum and urodeum cloacal chambers are separated by a narrower uroprocodeal fold with smooth muscle contraction capability. If cloacal contraction during intromission is purely reflexive or may have a voluntary component is unclear, but pertinent to understanding the potential cryptic female choice during copulation. The expansion of the glans ridge may aid to maintain intromission by allowing the female to constrict the fold and "grasp" the neck of the more bulbous glans. Therefore, the structurally robust dense, connective tissues of the glans ridge connected to the midline septum bisecting the expanded lumen may bolster the glans against vertical compression by the female cloaca. Further, a tight seal of the female cloaca on the base of the phallic glans may also act to exclude water from entering the urodeum during gamete transfer (Grigg and Kirshner, 2015). Taken together, both of these actions would be beneficial for animals that often copulate while floating in water.

While glans expansion may aid in maintaining intromission, it does not explain the distal structural elaborations. For example, the glans ridge has a midline crest that leads to a distal groove and the expanded glans has a distinct lateral notch. It is unclear with what parts of the female cloaca these features interact.

Oviducts of female crocodylians open to the dorsolateral, posterior aspect of the urodeum, each via a separate short vagina. The male Nile crocodile glans tip extends past the main body of the glans, has a medial bending, and a relatively blunt distal termination of the sulcus spermaticus. It has inflatable tissues throughout, so some aspect of rigidity seems to be required for normal function. From this initial morphological assessment, this structure seemingly does not focus the ejaculate or may not have sufficient length or lateral flexibility to enter or specifically direct ejaculate into the female vaginas. However, further detailed studies on male-female tissue interactions are clearly needed to better inform this research direction.

On both gross and histological levels, the glans is clearly more elaborate than the shaft. From proximal to distal, transverse sections show a decrease in dense connective tissue proportion, an introduction of lateral epithelium folds, and an increase of elastin fiber-rich tissues all contribute to allowing glans expansion, a biomechanical shift from rigidity to dynamic pliability.

Histological examination of the semen-conducting deep sulcus morphology lends cues about function. The tissue shows signs of the capability for substantial expansion during ejaculation as seem in the folded, branched epithelium surrounded by elastic fiber-rich tissues. In contrast, an outermost layer of dense connective tissues may serve to simultaneously protect from collapse and limit expansion during ejaculation; therefore, they work to promote fluid flow and maintain semen pressure as the liquid moves through the expanded sulcus.

These animals were collected from a commercial operation utilizing communal housing pens. Therefore, animals were held at increased densities than may be found in the wild, but no animals in the given groups had yet achieved sexual maturity. To varying degrees, we observed signs of penile skin infections associated with glans folds in all animal tissues histologically sectioned. These sites were characterized by eroded epithelium with subjacent aggregates of putative lymphocytes within the connective tissue stroma. Similar lymphoid follicles have previously been characterized on the penis of male alligators collected from farmed animals (Govett et al., 2005; Shilton et al., 2016).

The technique utilized in this manuscript to artificially inflate and fix phallic tissues in an approximated copulatory condition for measurement and histological analysis aided in dynamically understanding the Nile crocodile tissues examined. It could equally be applied to other crocodylian species to understand species-specific functional morphologies and highlight differences that underlie functional variation in copulatory interactions.

ACKNOWLEDGMENTS

This research was funded by a Sewanee faculty research grant. Many thanks to Mr. Stefan van As, managing director of Le Croc breeding farm and tannery, for his ongoing assistance with Nile crocodile research. This work was performed in collaboration with South African Crocodile Industry Association (SACIA) and Prof. Gerry Swan, Director of the Exotic Leather Research Centre (ELRC) of the University of Pretoria. Thank you to Prof. John Soley for his expertise and support.

REFERENCES

Brennan P.L.R., Clark C.J., Prum R.O. 2010. Explosive eversion and functional morphology of the duck penis supports sexual conflict in waterfowl genitalia. *Proceedings of the Royal Society B: Biological Sciences* 277:1309–1314. DOI

Fitri W.N., Wahid H., Rinalfi P.T., Rosnina Y., Raj D., Donny Y., … Malek A.A.A. 2018. Digital massage for semen collection, evaluation and extension in Malaysian estuarine crocodile (*Crocodylus porosus*). *Aquaculture* 483:169–172. DOI

Gist D.H., Bagwill A., Lance V., Sever D.M., Elsey R.M. 2008. Sperm storage in the oviduct of the American alligator. *Journal of Experimental Zoology Part A: Ecological Genetics and Physiology* 309:581–587. DOI

Govett P.D., Harms C.A., Johnson A.J., Latimer K.S., Wellehan J.F.X., Fatzinger M.H., … Lewbart G.A. 2005. Lymphoid follicular cloacal inflammation associated with a novel herpesvirus in juvenile alligators (*Alligator mississippiensis*). *Journal of Veterinary Diagnostic Investigation* 17:474–479. DOI

Gredler M.L. 2016. Developmental and evolutionary origins of the amniote phallus. *Integrative and Comparative Biology* 56:694–704. DOI

Grigg G., Kirshner D. 2015. Biology and Evolution of Crocodylians. Comstock Publishing Associates, Ithaca.

Johnston S.D., Lever J., McLeod R., Oishi M., Qualischefski E., Omanga C., … D'Occhio M. 2014. Semen collection and seminal characteristics of the Australian saltwater crocodile (*Crocodylus porosus*). *Aquaculture* 422–423:25–35. DOI

Kelly D.A. 2013. Penile anatomy and hypotheses of erectile function in the American alligator (*Alligator mississippiensis*): muscular eversion and elastic retraction. *The Anatomical Record* 296:488–496. DOI

Kelly D.A. 2016. Intromittent organ morphology and biomechanics: defining the physical challenges of copulation. *Integrative and Comparative Biology* 56:705–714. DOI

Kuchel L.J., Franklin C.E. 2000. Morphology of the cloaca in the estuarine crocodile, *Crocodylus porosus,* and its plastic response to salinity. *Journal of Morphology* 245:168–176. DOI

Moore B.C., Kelly D.A. 2015. Histological investigation of the adult alligator phallic sulcus. *South American Journal of Herpetology* 10:32–40. DOI

Moore B.C., Mathavan K., Guillette L.J. Jr. 2012. Morphology and histochemistry of juvenile male American alligator (*Alligator mississippiensis*) phallus. *The Anatomical Record* 295:328–337. DOI

Moore B.C., Spears D., Mascari T., Kelly D.A. 2016. Morphological characteristics regulating phallic glans engorgement in the American alligator. *Integrative and Comparative Biology* 56:657–668. DOI

Shilton C.M., Jerrett I.V., Davis S., Walsh S., Benedict S., Isberg S.R., … Melville L. 2016. Diagnostic investigation of new disease syndromes in farmed Australian saltwater crocodiles (*Crocodylus porosus*) reveals associations with herpesviral infection. *Journal of Veterinary Diagnostic Investigation* 28:279–290. DOI

Ziegler T., Olbort S. 2007. Genital structures and sex identification in crocodiles. *Crocodile Specialist Group Newsletter* 26:16–17.

ONLINE SUPPORTING INFORMATION

The following Supporting Information is available for this article online:

Video S1. Artificial inflation of the crocodile glans.